ISSN 1674-1056
http://cpb.iphy.ac.cn
http://iopscience.iop.org/cpb
中国物理 B
Chinese Physics
中国物理
Chinese Physics B

Laser cooling of CH molecule:Insights from *ab initio* study

Jie Cui(崔洁), Jian-Gang Xu(徐建刚), Jian-Xia Qi(祁建霞), Ge Dou(窦戈), Yun-Guang Zhang(张云光)
Citation: Chin. Phys. B . 2018, 27(10): 103101. **doi:** 10.1088/1674-1056/27/10/103101

Journal homepage: http://cpb.iphy.ac.cn; http://iopscience.iop.org/cpb

What follows is a list of articles you may be interested in

Theoretical study of spin-forbidden cooling transitions of indium hydride using *ab initio* methods

Yun-Guang Zhang(张云光), Hua Zhang(张华), Ge Dou(窦戈)
Chin. Phys. B . 2017, 26(9): 093101. **doi:** 10.1088/1674-1056/26/9/093101

Low-lying electronic states of CuN calculated by MRCI method

Shu-Dong Zhang(张树东), Chao Liu(刘超)
Chin. Phys. B . 2016, 25(10): 103103. **doi:** 10.1088/1674-1056/25/10/103103

Ab initio investigation of sulfur monofluoride and its singly charged cation and anion in their ground electronic state

Song Li(李松), Shan-Jun Chen(陈善俊), Yan Chen(陈艳), Peng Chen(陈朋)
Chin. Phys. B . 2016, 25(3): 033101. **doi:** 10.1088/1674-1056/25/3/033101

Globally accurate *ab initio* based potential energy surface of $H_2O^+(X^4A'')$

Song Yu-Zhi, Zhang Yuan, Zhang Lu-Lu, Gao Shou-Bao, Meng Qing-Tian
Chin. Phys. B . 2015, 24(6): 063101. **doi:** 10.1088/1674-1056/24/6/063101

Spectroscopic properties and radiative lifetimes of SiTe：A high-level multireference configuration interaction investigation

Li Rui, Zhang Xiao-Mei, Jin Ming-Xing, Xu Hai-Feng, Yan Bing
Chin. Phys. B . 2014, 23(5): 053101. **doi:** 10.1088/1674-1056/23/5/053101

Laser cooling of CH molecule: Insights from *ab initio* study*

Jie Cui(崔洁), Jian-Gang Xu(徐建刚), Jian-Xia Qi(祁建霞), Ge Dou(窦戈), and Yun-Guang Zhang(张云光)†

School of Science, Xi'an University of Posts and Telecommunications, Xi'an 710121, *China*

(Received 21 March 2018; revised manuscript received 25 July 2018; published online 10 September 2018)

The feasibility of laser cooling a CH molecule is investigated theoretically by employing the *ab initio* method. The potential energy curves for the five Λ–S states and eight Ω states of CH are determined by the multi-reference configuration interaction with the Davidson corrections (MRCI+Q) level of theory. The results agree well with the available experimental data and other theoretical values. Also, the permanent dipole moments and transition dipole moments of the CH molecule are calculated at the multi-reference configuration interaction (MRCI) level. We find highly diagonally distributed Franck–Condon factors ($f_{00} = 0.9950$ and 0.9998) and branching ratios ($R_{00} = 0.983$ and 0.993) for the $A^2\Delta \rightarrow X^2\Pi$ and $C^2\Sigma^+ \rightarrow X^2\Pi$ transitions. Moreover, the values of suitable radiative lifetime τ of the $A^2\Delta$ and $C^2\Sigma^+$ states are evaluated to be 9.64×10^{-7} s and 2.02×10^{-7} s, respectively, for rapid laser cooling. A scheme for laser cooling the CH molecule is designed. In the proposed cooling scheme, three wavelengths for $A^2\Delta \rightarrow X^2\Pi$ and $C^2\Sigma^+ \rightarrow X^2\Pi$ transitions are used, and the main pump lasers are $\lambda_{00} = 430.86$ nm and 313.45 nm, respectively. The feasibility of laser cooling the CH molecules is demonstrated for each of these schemes, and this study offers a theoretical basis for experimental research into preparation of cold CH molecules.

Keywords: spectroscopic constants, transition diople moments, Franck–Condon factors, laser cooling

PACS: 31.15.A–, 37.10.Mn, 87.80.Cc **DOI:** 10.1088/1674-1056/27/10/103101

1. Introduction

The production of ultracold polar molecules can be useful in several emerging fields such as quantum simulation,[1,2] chemical dynamics,[3] and new platforms for quantum computing,[4] as well as in controlling chemistry.[5] Consequently, the interest in potential molecular candidates for laser cooling has grown in response to the commencement of investigation and experimental research in this field. As early as 2004, Di Rosa[6] conducted a brief survey of candidate molecules for laser cooling and identified a series of hydrides and halides, including CaH, AlH, AlF, AlCl, etc. However, it was thought to be difficult to directly laser cool molecules because of their complex structures until the direct laser cooling of SrF molecules was first achieved and reported by Shuman *et al.* in 2010.[7] Since then, successful laser cooling experiments have been performed for YO, CaF, BH, and BaH.[8–12] Based on existing investigations, it can be concluded that molecular candidates for laser cooling must possess highly-diagonal Franck–Condon factors (FCFs) and short radiative lifetimes. In practice, highly-diagonal FCFs mean that a limited number of lasers is required to keep the molecule in a closed-loop cooling cycle, and short lifetimes can ensure high spontaneous emission.

Very recently, laser cooling of diatomic polar molecules and molecular ions has begun to attract the attention of researchers. In published research, it was predicted that some alkaline-earth-metal hydrides and halides, such as BeH, MgH, BeCl, could be laser-cooled.[13–17] These molecules have one thing in common: they have no intervening state between the proposed transition for the laser cooling. Therefore, it is necessary to ensure that if an intervening state exists, there is nonetheless closed cycling between the upper state and the ground state of the transition. The $A^1\Pi \rightarrow X^1\Sigma^+$ and $a^3\Pi \rightarrow X^1\Sigma^+$ transitions of AlF were studied by Wells and Lane,[18] these two transitions both have highly diagonal FCFs, and the lifetimes are also extremely short. Fortunately, the emission rate of $a^3\Pi$ state is very small. Soon after this study, laser cooling of the SiO^+ molecular ion was investigated by Nguyen and Odom[19] who found that between $B^2\Sigma^+$ and $X^2\Sigma^+$ states, there exits an intervening state, $A^2\Sigma^+$, but, due to its short lifetime, this did not prohibit the possibility of laser cooling. Following the publication of this study, increasing numbers of reports[20] of similar molecules, in which there exist intervening states, have provided bases for further research.

Here in this research, we report the accurate calculation of spectroscopic parameters and transition properties for the CH molecule to ensure its suitability for laser cooling. The CH radical occurring ubiquitously in interstellar space,[21] and high-power laser photochemistry[22] have been the subjects of numerous theoretical and experimental investigations. The experimental values of spin–orbit splitting for the $X^2\Pi$ and $A^2\Delta$ states of the CH molecule are 27.95 cm^{-1} and 1.0 cm^{-1}, respectively, which were derived by Huber and Herzberg,[23] in 1979. In recent years, the spectroscopic constants of the $X^2\Pi$ and $A^2\Delta$ states were calculated by using different theoretical methods.[24–27] In 2003, Sun and Freed[28] used an *ab initio*

*Project supported by the National Natural Science Foundation of China (Grant No. 61705182).

†Corresponding author. E-mail: zygsr2010@163.com

© 2018 Chinese Physical Society and IOP Publishing Ltd

effective valence shell Hamiltonian method to carry out a theoretical investigation of the spin–orbit splitting, and their results for the energies of these two states are 33.96 cm^{-1} and 1.27 cm^{-1}, respectively. In these previous theoretical and experimental studies,[24–27,29–34] for the $A^2\Delta \rightarrow X^2\Pi$ transition, the region of transition energy (T_e) from the $A^2\Delta$ state to the $X^2\Pi$ state was between 23147.884 cm^{-1} and 23565.4 cm^{-1}; for the $C^2\Sigma^+ \rightarrow X^2\Pi$ transition, the region of T_e was from 31802.128 cm^{-1} to 32205.44 cm^{-1}. However, to the best of our knowledge, a systematic study of the laser cooling of CH is unavailable so far. The objective of the present work is to design a viable scheme to facilitate the laser cooling of the CH molecule, including computation of permanent dipole moments (PDMs), transition dipole moments (TDMs), FCFs, radiative lifetimes, and wavelengths for the $A^2\Delta \rightarrow X^2\Pi$ and $C^2\Sigma^+ \rightarrow X^2\Pi$ transitions of CH molecule by using a high-level *ab initio* method.

The rest of this paper is arranged as follows. In Section 2, we detail the *ab initio* method and basis sets chosen in the presented calculations of the electronic states of CH molecules. The results of the spectroscopic parameters obtained for the Λ–S and Ω states and laser cooling for the Λ–S states of CH are provided and discussed in Section 3. Finally, some conclusions are given in Section 4.

2. Computational details

By using the MOLPRO 2015 program package,[35] all electronic structures of CH molecules for the $X^2\Pi$, $a^4\Sigma^-$, $A^2\Delta$, $B^2\Sigma^-$, and $C^2\Sigma^+$ states are calculated. In the first step we used the Post restricted Hartree–Fock (RHF) method to calculate the energy for the ground state. The next step was to obtain a multi-reference wavefunction by using the complete active space self-consistent-field (CASSCF) method.[36–38] The final step was based on the zero-order function, by using the multi-reference configuration interaction (MRCI) plus Davidson corrections (MRCI+Q) to calculate energies for the CH molecule,[39–42] and taking advantage of the Douglas–Kroll (DHK) method for correction.[43–45] The spin–orbit coupling (SOC) effects were also taken into consideration in the MRCI+Q calculations of the CH molecule.

Due to the limitation of the summary of the MOLPRO program package, the computations were performed within the C_{2v} point group symmetry, which has four irreducible representations (irreps) (A_1, B_1, B_2, and A_2). The A_1 irrep yields the Σ^+ state and a component of Δ states, B_1 provides the Π state, and A_2 yields the Σ^- state and the other components of Δ states. In the CASSCF calculations, six molecule orbitals are chosen as the active space, including four A_1, one B_1, and one B_2. Five electrons are distributed in the (4110) active space. The aug-cc-pV5Z basis set is chosen for the hydrogen atom, and the aug-cc-pCV5Z basis set is for the carbon atom. In all electronic structure calculations, the aug-cc-pCV5Z (ACV5Z) basis set is used for the Λ–S and Ω states.

For the bound Λ–S and Ω states, all potential energy curves (PECs) are calculated with an interval of 0.05 nm over the distance of 0.04 nm–1.5 nm. To achieve the accurate results, the interval value is reduced to 0.02 nm, nearly the equilibrium bond distance. The spectroscopic constants are calculated by solving the nuclear Schrödinger equation through using the LEVEL 8.2 program, including the equilibrium bond length, R_e, harmonic and an harmonic vibrational constants, ω_e and $\omega_e\chi_e$, respectively, rotational constant, B_e, and adiabatic relative electronic energy referred to the ground state, T_e.[46] With the PECs and TDMs of the different electronic states, this program can also yield the FCFs and Einstein coefficients for all possible discrete transitions allowed by selection rules. The Einstein coefficient $A_{v'v}$ for the rate of spontaneous emission from an initial rovibrational level (v, J) into the final rovibrational level (v', J') is defined by the expression[47]

$$A_{v'v} = 3.1361891 \times 10^{-7} \frac{S(J',J)}{2J'+1} \Delta E_{v',v}^3 \left| \left\langle \psi_{v'J'} \left| M(r) \right| \psi_{vJ} \right\rangle \right|^2, \quad (1)$$

where $M(r)$ is the function of transition dipole in units of D, v is the emission frequency, $\psi_{v'J'}$ and ψ_{vJ} are the normalized radial wavefunctions, the energy difference $\Delta E_{v'v}$ is in units of cm^{-1}, and $S(J', J)$ is the Hönl–London rotational intensity factor.[48,49] Using the Einstein coefficient for spontaneous emission, the radiative lifetime can be calculated from the following formula:

$$\tau = 1/\sum\nolimits_v A_{v'v}. \quad (2)$$

3. Results and discussion

3.1. PECs and spectroscopic constants of Λ–S states

To determine whether the CH molecule is suitable for laser cooling, we must calculate the PECs and spectroscopic constants. At the MRCI+Q level, the CH molecule for the lowest two dissociation channels, $C(^3P) + H(^2S)$ and $C(^1D) + H(^2S)$, and the $X^2\Pi$, $a^4\Sigma^-$, $A^2\Delta$, $B^2\Sigma^-$, and $C^2\Sigma^+$ states are obtained. Figure 1 shows the PECs for the Λ–S states of the CH molecule. The associated sets of calculated spectroscopic parameters with available experimental data[29–34] and theoretical results[24–27] of CH are summarized in Table 1 for comparison.

As for the ground state $X^2\Pi$, the equilibrium bond distance and the vibrational frequency are calculated to be R_e = 1.1181 Å and ω_e = 2859.4759 cm^{-1}, and their corresponding differences from experimental values are only 0.0019 Å and 1.3241 cm^{-1}, respectively:[29,30] the percentage errors are only 0.17% and 0.05%, respectively. Compared with other theoretical values[24–27] of $\omega_e\chi_e$ and B_e, our constants $\omega_e\chi_e$ =

62.3206 cm^{-1} and $B_e = 14.5084$ cm^{-1} are in good accordance with the experimental data of 64.4 cm^{-1} and 14.457 cm^{-1}. Our computed value for D_e is 3.669 eV, while the experimental value is 3.472 eV, and the percentage error is 5.67%. For the second singlet excited state $B^2\Sigma^-$, in the case of the spectroscopic constants R_e, and T_e, our data, 1.1624 Å, 26007.57 cm^{-1}, respectively, are in better agreement with the experimental data (1.164 Å, 26059.517 cm^{-1}) than those of other published calculations.[32,33] The value of ω_e that we computed for the $B^2\Sigma^-$ state is larger than the experimental measurement, giving a percentage error of 20.67%, but is in good agreement with other theoretical values, and the corresponding percentage error, between our theoretical value and others in the literature, for the $B^2\Sigma^-$ state is 0.05% (Ref. [24]) $\leq \delta\omega_e/\omega_e \leq$ 1.85% (Ref. [25]).

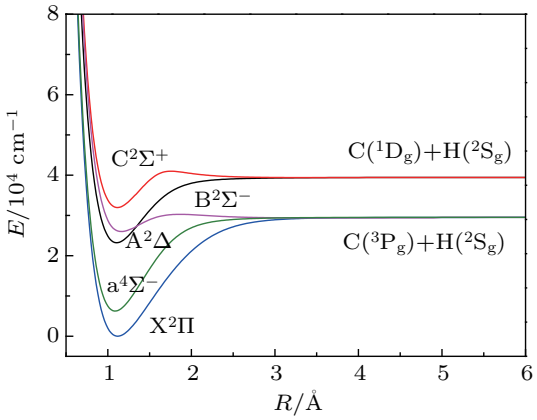


Fig. 1. (color online) PECs for the five Λ–S states of CH molecule.

Table 1. Spectroscopic constants for Λ–S states of CH molecule at MRCI+Q level.

		R_e/Å	ω_e/cm^{-1}	$\omega_e\chi_e$/cm^{-1}	B_e/cm^{-1}	T_e/cm^{-1}	D_e/eV
X$^2\Pi$	Present	1.1181	2859.48	62.32	14.5084	0	3.669
	Ref. [27]	1.122	2882.50	54.70	14.4	–	3.399
	Ref. [24]	1.12	2851.00	62.20	–	–	3.447
	Ref. [25]	1.123	2863.10	73.10	–	–	3.413
	Ref. [26]	1.124	2851.90	66.60	–	–	–
	Expt.[29,30]	1.120	2860.80	64.40	14.457	0	3.472
a$^4\Sigma^-$	Present	1.0872	3200.59	90.82	15.3343	6245.28	2.894
	Ref. [27]	1.091	3158.50	71.40	15.2	–	2.688
	Ref. [24]	1.090	3090.90	102.20	–	6024.902	2.676
	Ref. [25]	1.093	3085.10	68.00	–	5847.462	2.680
	Ref. [26]	1.091	3117.30	80.60	–	5778.7	–
	Expt.[29]	1.085	3145.00	72.00	15.4	5844	–
A$^2\Delta$	Present	1.1032	2967.23	105.61	14.9166	23280.16	2.024
	Ref. [24]	1.106	2911.10	91.99	–	23395.07	1.801
	Ref. [25]	1.109	2888.80	82.80	–	23510.83	1.760
	Ref. [26]	1.107	2926.90	103.80	–	23565.4	–
	Expt.[30,31]	1.103	2914.10	96.65	14.934	23147.88	1.836
B$^2\Sigma^-$	Present	1.1624	2166.01	161.11	13.5087	26007.57	0.438
	Ref. [24]	1.175	2167.10	173.70	–	26140.17	0.244
	Ref. [25]	1.181	2126.70	198.60	–	26204.69	0.209
	Expt.[32,33]	1.164	1794.90	225.70	12.645	26059.52	0.305
C$^2\Sigma^+$	Present	1.1155	2867.18	128.26	14.626	31961.97	0.930
	Ref. [24]	1.116	2837.30	87.760	–	32124.75	0.738
	Ref. [25]	1.122	2781.50	115.20	–	32205.40	0.738
	Ref. [26]	1.118	2853.30	133.00	–	32184.7	0.749
	Expt.[29,34]	1.114	2840.20	126.00	14.603	31802.13	0.769

For the first singlet excited state $A^2\Delta$ of the higher dissociation channel $C(^1D) + H(^2S)$, shown in Fig. 1, the calculated T_e from the $X^2\Pi$ state is located at 23280.16 cm^{-1}. Our result of $\omega_e = 2967.2279$ cm^{-1} is a little overestimated with respect to the experimental and other theoretical results, the percentage error is 1.36% (Ref. [26]) $\leq \delta\omega_e/\omega_e \leq$ 2.71% (Ref. [25]). Our value of R_e is 1.1032 Å which is 0.0002 Å larger than the experimental value. The value of T_e from experiments[30,31] is 23147.884 cm^{-1}, in other theoretical results it is 23395.072 cm^{-1},[24] 23510.830 cm^{-1},[25] 23565.4 cm^{-1},[26] as reported by Kalemos *et al.,* Kleinschmidt *et al.*, and Hettema and Yarkony, respectively. Obviously, our value of T_e is much closer to the experimental value than the other theoretical ones, the corresponding error relative to the experimental value is only 0.57%. For the third excited singlet $C^2\Sigma^+$ state, our values of R_e, $\omega_e\chi_e$, B_e, and T_e are much closer to the experimental data than theoretical ones reported by Richards *et al.*[29] and Herzberg *et al.*[34] Specifically, the

differences between the experimental value and our value are only 0.0015 Å for R_e and 0.023 cm^{-1} for B_e, respectively. We also notice that the error for the present result of $C^2\Sigma^+$ is a little larger than the experimental data. For example, our results for R_e, $\omega_e\chi_e$, B_e are 1.1155 Å, 128.2555 cm^{-1}, and 14.626 cm^{-1}, and the experimental values are 1.114 Å, 126 cm^{-1}, and 14.603 cm^{-1}, respectively. Obviously, the differences are very small; the percentage errors are 0.13%, 1.79%, and 0.16%, respectively. Concerning the quartet state, both previous studies and our present one obtain spectroscopic parameters for the $a^4\Sigma^-$state of the CH molecule. Compared with the theoretical data,[24–27] our results for the $a^4\Sigma^-$ state are in good agreement. For instance, our value of $\omega_e = 3200.5941$ cm^{-1} is a little larger than the theoretical values in the literature, with a percentage error being 2.67%–3.74% for this difference; our result of R_e is 1.0872 Å, and the percentage error for this value is 0.26% (Ref. [24]) $\leq \delta R_e/R_e \leq 0.53\%$ (Ref. [25]).

In conclusion, our spectroscopic parameter results agree with those of the experimental data and theoretical results in terms of the $X^2\Pi$, $a^4\Sigma^-$, $A^2\Delta$, $B^2\Sigma^-$, and $C^2\Sigma^+$ states of CH.

3.2. PECs and spectroscopic constants of Ω states

For the CH molecule, the spin–orbit coupling (SOC) effect makes the five Λ–S states split into eight Ω states, i.e. four $\Omega = 1/2$ states, three $\Omega = 3/2$ states, and one $\Omega = 5/2$ state. Four new dissociation limits,$C(^3P_0) + H(^2S_{1/2})$,$C(^3P_1) + H(^2S_{1/2})$, $C(^3P_2) + H(^2S_{1/2})$, and $C(^1D_2) + H(^2S_{1/2})$ are generated from the original $C(^3P) + H(^2S)$ and $C(^1D) + H(^2S)$ limits. The PECs for $X^2\Pi_{1/2}$, $X^2\Pi_{3/2}$, $a^4\Sigma^-_{1/2}$, $a^4\Sigma^-_{3/2}$, $A^2\Delta_{3/2}$, $A^2\Delta_{5/2}$, $B^2\Sigma^-_{1/2}$, and $C^2\Sigma^+_{1/2}$ states are plotted in Fig. 2, and the corresponding spectroscopic parameters for the eight Ω states are listed in Table 2.

Table 2. Spectroscopic constants of various bound Ω states of CH molecule.

	R_e/Å	ω_e/cm^{-1}	$\omega_e\chi_e$/cm^{-1}	B_e/cm^{-1}	T_e/cm^{-1}	D_e/eV
$X^2\Pi_{1/2}$	1.1179	2856.39	61.56	14.5088	0	3.654
$X^2\Pi_{3/2}$	1.1179	2856.63	61.58	14.5093	26.81	3.652
$a^4\Sigma^-_{1/2}$	1.0875	3196.06	90.46	15.3356	6168.91	2.890
$a^4\Sigma^-_{3/2}$	1.0875	3196.06	90.46	15.3356	6168.95	2.891
$A^2\Delta_{3/2}$	1.1040	2935.27	138.61	15.0553	23358.32	1.999
$A^2\Delta_{5/2}$	1.1040	3121.79	109.32	14.9152	23361.23	1.985
$B^2\Sigma^-_{1/2}$	1.1850	2166.83	182.62	13.3591	26189.11	0.403
$C^2\Sigma^+_{1/2}$	1.1141	2858.66	121.07	14.6380	31961.73	0.932

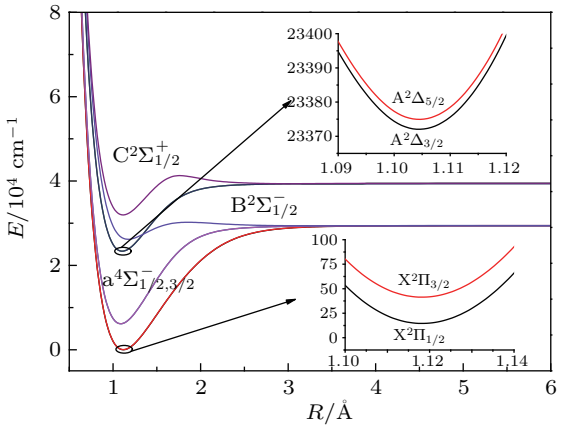


Fig. 2. (color online) PECs for eight Ω states for the CH molecule.

As we can see from Table 2, the effects of SOC are weak on the spectroscopic constants for $X^2\Pi$, $a^4\Sigma^-$, $B^2\Sigma^-$, and $C^2\Sigma^+$ states, but the effect of SOC is great for the $A^2\Delta$ state. For the $B^2\Sigma^-_{1/2}$ state, the spectroscopic parameters are in excellent agreement with the corresponding values without considering the SOC effect; the differences are only 0.8286 cm^{-1} and 0.1496 cm^{-1} for ω_e and B_e, respectively. Our calculated spectroscopic parameters for the $C^2\Sigma^+_{1/2}$ state are $R_e = 1.1141$ Å, $\omega_e = 2858.6584$ cm^{-1}, $\omega_e\chi_e = 121.0729$ cm^{-1}, $B_e = 14.6380$ cm^{-1}, and $T_e = 31961.73$ cm^{-1}, which differ from the corresponding values computed without considering the SOC effect by only 0.001 Å, 8.5189 cm^{-1}, 7.1826 cm^{-1}, and 0.24 cm^{-1}, respectively.

Owing to the SOC effect, the Λ–S $X^2\Pi$ state splits into two $X^2\Pi_{1/2}$ and $X^2\Pi_{3/2}$ states. For the two Ω states, the energy sequence from low to high is 1/2, 3/2, and the small difference of T_e between the states is 26.81 cm^{-1}. By comparing the $X^2\Pi$ state and the $X^2\Pi_{1/2}$, $X^2\Pi_{3/2}$ states in Table 1 and Table 2, it can be seen that the spectroscopic parameters of the states $X^2\Pi_{1/2}$ and $X^2\Pi_{3/2}$ are similar to those of the $X^2\Pi$ state. For example, the differences between the values of ω_e in the Ω states of $X^2\Pi_{1/2}$ and $X^2\Pi_{3/2}$ and that of the $X^2\Pi$ state are only 3.0881 cm^{-1} and 2.8474 cm^{-1}. The values of $\omega_e\chi_e$ for the $X^2\Pi_{1/2}$ and $X^2\Pi_{3/2}$ states are only 0.7577 cm^{-1} and 0.7456 cm^{-1} smaller than the value for the $X^2\Pi$ state, respectively. For the $a^4\Sigma^-$ state, which splits into two Ω states ($a^4\Sigma^-_{1/2}$, $a^4\Sigma^-_{3/2}$), the spectroscopic data for the two Ω states are almost the same as the constants of the Λ–S state, and the difference in T_e between the two Ω states is 0.04 cm^{-1}. As for $\omega_e\chi_e$ and B_e of the two Ω states, the largest differences of the $a^4\Sigma^-$ state are 0.3602 cm^{-1} and 0.0013 cm^{-1}, respectively.

The difference in T_e between $A^2\Delta_{3/2}$ and $A^2\Delta_{5/2}$ is 2.91 cm^{-1}. However, we also notice that the SOC effect is very large for the $A^2\Delta$ state. As Table 2 shows, the two Ω states have the values of both ω_e and $\omega_e\chi_e$, which are quite different, the percentage differences are 5% and 21%, respectively. In addition, between these two Ω states, the difference in T_e is 2.91 cm^{-1}.

3.3. PDMs and TDMs

PDMs for the $X^2\Pi$, $a^4\Sigma^-$, $A^2\Delta$, $B^2\Sigma^-$, and $C^2\Sigma^+$ states are plotted in Fig. 3. As we can see from Fig. 3, the maximum PDM exhibited by the $X^2\Pi$ state is much larger than the others, which is due to the deepest potential well of the ground state. For the ground state, the value reaches a maximum of about 0.7421 a.u. (the unit a.u. is short for atomic unit), and then drops to a minimum at 2.28 Å. Furthermore, the PDMs increase linearly up to approximately 2.34 Å. As for the $C^2\Sigma^+$ state, a maximum and a minimum also exist of the PDM at 1.4 Å and 2.12 Å, respectively. It can be clearly seen from Fig. 3 that the PDMs for the $a^4\Sigma^-$, $A^2\Delta$, and $B^2\Sigma^-$ states each have a similar trend, their maximum values being 0.3591, 0.4379, and 0.5466 a.u., respectively. Then, the PDMs of these states then all drop to zero when moving to approximately 4.8 Å. The PDM functions of the $X^2\Pi$, $a^4\Sigma^-$, $A^2\Delta$, $B^2\Sigma^-$, and $C^2\Sigma^+$ states at R_e are 0.4981, 0.2408, 0.2825, 0.5089, and 0.3505 a.u., respectively.

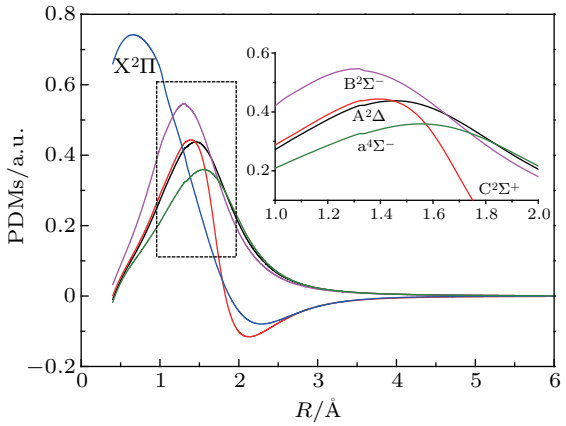


Fig. 3. (color online) PDMs for five Λ–S states of CH molecule.

The TDMs for the $A^2\Delta \rightarrow X^2\Pi$, $B^2\Sigma^- \rightarrow X^2\Pi$, and $C^2\Sigma^+ \rightarrow X^2\Pi$ transitions as a function of the internuclear distance at the MRCI+Q level for the CH molecule are plotted in Fig. 4. There are intermediate states in $A^2\Delta \rightarrow X^2\Pi$ and $C^2\Sigma^+ \rightarrow X^2\Pi$ transitions. So it is necessary to study the influence of the intermediate state. For $A^2\Delta \rightarrow X^2\Pi$, the intermediate state $a^4\Sigma^-$ has no effect on the transition, because the $A^2\Delta \rightarrow a^4\Sigma^-$ transition is spin–orbit forbidden. Between the $X^2\Pi$ and $C^2\Sigma^+$, the intermediate states are $a^4\Sigma^-$, $A^2\Delta$, and $B^2\Sigma^-$. However, the transition of $C^2\Sigma^+ \rightarrow a^4\Sigma^-$ is spin–orbit forbidden. The TDMs for $C^2\Sigma^+ \rightarrow A^2\Delta$ transition are about zero due to being orbit-forbidden and for the $C^2\Sigma^+ \rightarrow B^2\Sigma^-$ transition they are about zero because the $\Sigma^+ \rightarrow \Sigma^-$ is forbidden, which shows that the two transitions are unfeasible. So neither the $a^4\Sigma^-$ nor $A^2\Delta$, nor $B^2\Sigma^-$ has an effect on the $C^2\Sigma^+ \rightarrow X^2\Pi$. Figure 4 shows that the TDMs for these three transitions fall to minima, after which these transitions rise, approaching zero with bond length increasing. In addition, the minimum of $C^2\Sigma^+ \rightarrow X^2\Pi$ transition is −0.03 Å, which is smaller than the other two transitions. The TDMs for the $A^2\Delta$, $B^2\Sigma^-$, and $C^2\Sigma^+$ states at R_e are 0.2102, 0.2364, and 0.2803 a.u., respectively. TDMs of the states are related to the Einstein coefficients and radiative lifetimes.

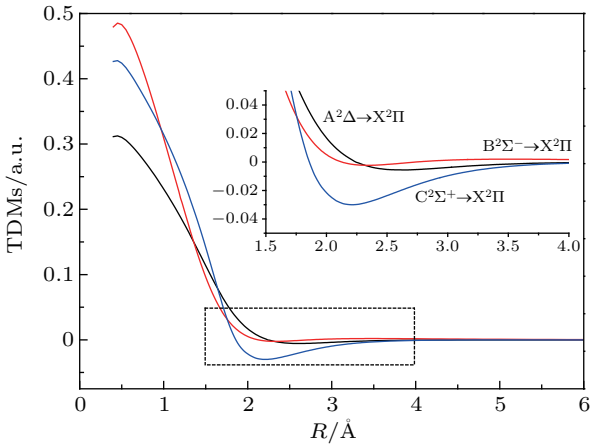


Fig. 4. (color online) TDMs for $A^2\Delta \rightarrow X^2\Pi$, $B^2\Sigma^- \rightarrow X^2\Pi$, and $C^2\Sigma^+ \rightarrow X^2\Pi$ transitions of CH molecule.

3.4. Laser cooling of CH

As mentioned in Section 1, one of the criteria for laser cooling is that the molecule must possess highly diagonal FCFs, which can be used to describe the transition by the degree of overlap of the vibrational wave functions. The splitting constants for $X^2\Pi$ and $A^2\Delta$ are small for CH, i.e. $A^{SO}(X^2\Pi_{1/2}$ and $X^2\Pi_{3/2}) = 26.81$ cm^{-1}, $A^{SO}(A^2\Delta_{1/2}$ and $A^2\Delta_{3/2}) = 2.91$ cm^{-1}. So the SOC effect for laser cooling the CH molecule can be ignored. The influences of intermediate states are also considered. Fortunately, these intermediate states have no effect on the $A^2\Delta \rightarrow X^2\Pi$ transition nor on the $C^2\Sigma^+ \rightarrow X^2\Pi$ transition as mentioned in the TDM part. Here, the possibility of laser cooling on the $A^2\Delta \rightarrow X^2\Pi$ transition and $C^2\Sigma^+ \rightarrow X^2\Pi$ transition are considered. As can be seen in Table 3, the diagonal FCFs are $f_{00} = 0.9950$ for the $A^2\Delta \rightarrow X^2\Pi$ transition and $f_{00} = 0.9998$ for the $C^2\Sigma^+ \rightarrow X^2\Pi$ transition, which can greatly limit the number of lasers required to keep the molecule in a closed-loop cooling cycle. Other calculated diagonal FCFs for $A^2\Delta \rightarrow X^2\Pi$ such as f_{11} (0.989), f_{22} (0.991), f_{33} (0.991), and for the $C^2\Sigma^+ \rightarrow X^2\Pi$ transition like f_{11} (0.997), f_{22} (0.970), f_{33} (0.777) are smaller than f_{00} but remain considerably large compared with the small off-diagonal terms. In addition, to demonstrate the distributions of FCFs for the different vibrational states of $A^2\Delta \rightarrow X^2\Pi$ and $C^2\Sigma^+ \rightarrow X^2\Pi$ transitions, all possible transitions between

$0 \leq v \leq 3$ and $0 \leq v' \leq 1$ are displayed in Table 3. Besides the large diagonal FCFs, another critical criterion for laser cooling a molecule is a suitable rate of optical cycling. This means that for the rapid laser cooling implementation, short spontaneous radiative lifetimes τ (10^{-8} s–10^{-5} s) are required. The values of corresponding computed spontaneous radiative lifetime τ are collected in Table 3. As illustrated in the table, the values of spontaneous radiative lifetime τ of the $A^2\Delta \rightarrow X^2\Pi$ and $C^2\Sigma^+ \rightarrow X^2\Pi$ transitions are 9.64×10^{-7} s and 2.02×10^{-7} s, respectively, which are suitable for laser cooling the CH molecule.

Comparing the relevant FCFs is a simple method of determining the cooling cycle, but it is not sufficient alone. The reason is that the relation between the relative strengths of the vibrational branching ratios and that between photon loss pathways are more direct than FCFs in the cooling cycle.[50–52] Thus, the cooling cycle with branching ratio $R_{v'v}$, which can be calculated by using the ratio of Einstein coefficients $A_{v'v}$ for each vibronic transition, is expressed as $R_{v'v} = A_{v'v}/\sum_v A_{v'v}$. The calculated values of Einstein coefficient $A_{v'v}$ and vibrational branching ratio $R_{v'v}$ of the $A^2\Delta \rightarrow X^2\Pi$ and $C^2\Sigma^+ \rightarrow X^2\Pi$ transitions are listed in Table 4. For the $A^2\Delta \rightarrow X^2\Pi$ transition, branching ratios of the diagonal terms $R_{00} = 0.983$ and $R_{11} = 0.968$ are obtained; branching ratios of the off-diagonal terms $R_{01} = 1.65 \times 10^{-2}$, $R_{02} = 4.27 \times 10^{-4}$, $R_{03} = 1.05 \times 10^{-5}$, $R_{10} = 5.39 \times 10^{-4}$, $R_{12} = 2.97 \times 10^{-2}$, and $R_{13} = 1.37 \times 10^{-3}$ are also calculated. The branching ratios to the $v \geqslant 3$ states of the CH molecule for the $A^2\Delta \rightarrow X^2\Pi$ transition are $R_{03+} \leq 3 \times 10^{-7}$, so a cyclic system with three lasers involving $v = 0$, 1, 2, 3 of the $X^2\Pi$ state and $v' = 0$ and 1 levels of the $A^2\Delta$ state is proposed, based on the calculated $R_{v'v}$. For the $C^2\Sigma^+ \rightarrow X^2\Pi$ transition, the diagonal terms R_{00} (0.993) and R_{11} (0.979) are a little smaller than f_{00} (0.999) and f_{11} (0.997). The value of R_{03} is 3.73×10^{-6}, which is larger than $f_{03}(4.04 \times 10^{-7})$. However, the value of R_{03} is small enough to make the $C^2\Sigma^+ \rightarrow X^2\Pi$ transition used as a quasi-cycling transition.

Table 3. Calculated values of FCF $f_{v'v}$, wavelength $\lambda_{v'v}$, and spontaneous radiative lifetime τ.

Transition	f_{00} f_{10}	f_{01} f_{11}	f_{02} f_{12}	f_{03} f_{13}	λ_{00}	λ_{01}	λ_{12}	τ/s
$A^2\Delta \rightarrow X^2\Pi$	0.9950 4.91×10^{-3}	4.76×10^{-3} 0.9888	2.70×10^{-4} 5.22×10^{-3}	2.98×10^{-6} 1.00×10^{-4}	430.86	488.20	484.78	9.64×10^{-7}
$C^2\Sigma^+ \rightarrow X^2\Pi$	0.9998 2.08×10^{-6}	1.22×10^{-6} 0.9967	2.00×10^{-4} 1.94×10^{-3}	4.04×10^{-7} 1.31×10^{-3}	313.45	342.73	342.61	2.02×10^{-7}

Table 4. Calculated values of Einstein coefficient $A_{v'v}$ and vibrational branching ratio $R_{v'v}$ of $A^2\Delta \rightarrow X^2\Pi$ and $C^2\Sigma^+ \rightarrow X^2\Pi$ transitions.

		$v = 0$		$v = 1$		$v = 2$		$v = 3$	
		$A_{v'v}$	$R_{v'v}$	$A_{v'v}$	$R_{v'v}$	$A_{v'v}$	$R_{v'v}$	$A_{v'v}$	$R_{v'v}$
$A^2\Delta \rightarrow X^2\Pi$	$v' = 0$	1.04×10^6	9.83×10^{-1}	1.74×10^4	1.65×10^{-2}	4.50×10^2	4.27×10^{-4}	1.11×10^1	1.05×10^{-5}
	$v' = 1$	5.19×10^2	5.39×10^{-4}	9.31×10^5	9.68×10^{-1}	2.86×10^4	2.97×10^{-2}	1.32×10^3	1.37×10^{-3}
$C^2\Sigma^+ \rightarrow X^2\Pi$	$v' = 0$	4.94×10^6	9.93×10^{-1}	3.38×10^4	6.79×10^{-3}	9.23×10^2	1.85×10^{-4}	1.86×10^1	3.73×10^{-6}
	$v' = 1$	5.16×10^4	1.17×10^{-2}	4.32×10^6	9.79×10^{-1}	3.98×10^4	9.01×10^{-3}	2.79×10^3	6.32×10^{-4}

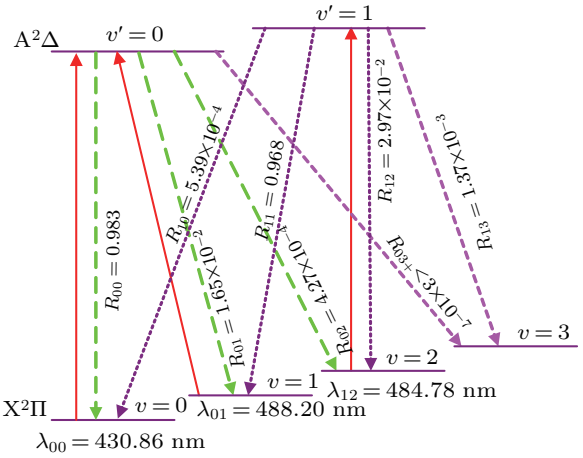


Fig. 5. (color online) Proposed laser cooling scheme for CH using $A^2\Delta(v') \rightarrow X^2\Pi(v)$ transition (solid red) and spontaneous decay (dotted line) with calculated values of $R_{v'v}$. Here $\lambda_{v'v}$ is the wavelength of $A^2\Delta(v') \rightarrow X^2\Pi(v)$ transition.

In Figs. 5 and 6, the two schemes show the arranged laser-driven transitions (solid red) and spontaneous decay (dotted line) for CH. As can be seen, the $A^2\Delta(v' = 0) \rightarrow X^2\Pi(v = 0)$ or $C^2\Sigma^+(v' = 0) \rightarrow X^2\Pi(v = 0)$ transitions are the main pumps for cooling the CH molecule, requiring a laser with wavelength $\lambda_{00} = 430.86$ nm or $\lambda_{00} = 313.45$ nm, respectively. To augment the cooling effect, two cycles are added with $A^2\Delta(v' = 0) \rightarrow X^2\Pi(v = 1)$ and $C^2\Sigma^+(v' = 0) \rightarrow X^2\Pi(v = 1)$ transitions, which are the first vibrational pump, and the $A^2\Delta(v' = 1) \rightarrow X^2\Pi(v = 2)$ and $C^2\Sigma^+(v' = 1) \rightarrow X^2\Pi(v = 2)$ transitions are the second vibrational pump. Furthermore, the wavelengths of the two additional lasers for the $A^2\Delta \rightarrow X^2\Pi$ transition are $\lambda_{01} = 488.20$ nm and $\lambda_{12} = 484.78$ nm; for the $C^2\Sigma^+ \rightarrow X^2\Pi$ transition their wavelengths are $\lambda_{01} = 342.73$ nm and $\lambda_{12} = 342.61$ nm.

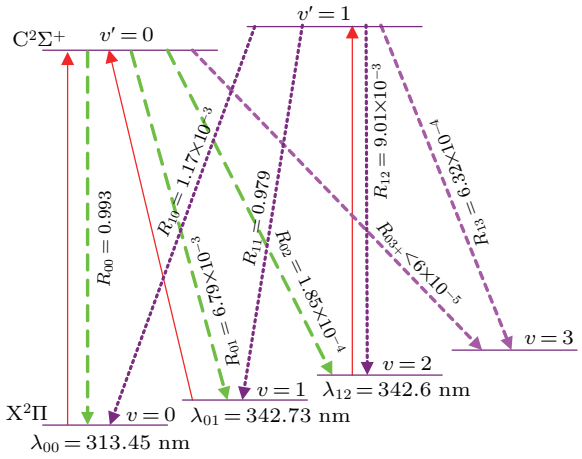


Fig. 6. (color online) Proposed laser cooling scheme for CH using the $C^2\Sigma^+(v')\rightarrow X^2\Pi(v)$ transition (solid red) and spontaneous decay (dotted line) with calculated values of $R_{v'v}$. Here $A_{v'v}$ is the wavelength of the $C^2\Sigma^+(v')\rightarrow X^2\Pi(v)$ transition.

4. Conclusions

The PECs for the Λ–S states $X^2\Pi$, $a^4\Sigma^-$, $A^2\Delta$, $B^2\Sigma^-$, and $C^2\Sigma^+$, and the Ω states $X^2\Pi_{1/2}$, $X^2\Pi_{3/2}$, $a^4\Sigma^-_{1/2}$, $a^4\Sigma^-_{3/2}$, $A^2\Delta_{3/2}$, $A^2\Delta_{5/2}$, $B^2\Sigma^-_{1/2}$, and $C^2\Sigma^+_{1/2}$ of the CH molecule have been investigated at the MRCI+Q level with the aug-cc-pCV5Z basis set. Using the Level 8.2 program to solve the nuclear Schrödinger equation, the results of spectroscopic constants for these Λ–S and Ω states are obtained. Furthermore, the results agree well with previous experimental and other theoretical values.

In Subsection 3.3, our computed PDMs, for the $X^2\Pi$, $a^4\Sigma^-$, $A^2\Delta$, $B^2\Sigma^-$, and $C^2\Sigma^+$ states, and TDMs, for the spin-allowed transitions $A^2\Delta\rightarrow X^2\Pi$, $B^2\Sigma^-\rightarrow X^2\Pi$, and $C^2\Sigma^+\rightarrow X^2\Pi$, are discussed. Based on PECs and TDMs that we obtained, the FCFs are calculated. The results indicate that the $A^2\Delta\rightarrow X^2\Pi$ and $C^2\Sigma^+\rightarrow X^2\Pi$ transitions have highly diagonal FCFs ($f_{00}=0.9950$ and 0.9998) and branching ratios ($R_{00}=0.983$ and 0.993). Suitable radiative lifetimes, $\tau=9.64\times10^{-7}$ s for the $A^2\Delta\rightarrow X^2\Pi$ transition and $\tau=2.02\times10^{-7}$ s for the $C^2\Sigma^+\rightarrow X^2\Pi$ transition, for ensuring the rapid and efficient laser cooling of the CH molecule are also obtained. The $a^4\Sigma^-\rightarrow X^2\Pi$ transition is prohibitive to laser cooling because it is forbidden by selection rules. An optical scheme consisting of three laser cycles with the $A^2\Delta\rightarrow X^2\Pi$ and $C^2\Sigma^+\rightarrow X^2\Pi$ transitions to create ultra cold CH molecules is proposed. The main cycling laser wavelengths for the $A^2\Delta(v'=0)\rightarrow X^2\Pi(v=0)$ and $C^2\Sigma^+(v'=0)\rightarrow X^2\Pi(v=0)$ transitions are $\lambda_{00}=430.86$ nm and 313.45 nm, respectively. To enhance the cooling effect, two additional lasers with $\lambda_{10}=488.20$ nm and $\lambda_{21}=484.78$ nm are required for the $A^2\Delta(v'=0)\rightarrow X^2\Pi(v=1)$ and $A^2\Delta(v'=1)\rightarrow X^2\Pi(v=2)$ transitions and $\lambda_{10}=342.73$ nm, $\lambda_{21}=324.61$ nm for $C^2\Sigma^+(v'=0)\rightarrow X^2\Pi(v=1)$, $C^2\Sigma^+(v'=1)\rightarrow X^2\Pi(v=2)$ transitions, respectively. The results indicate that laser cooling of the CH molecule is viable, and a reliable theoretical reference is provided for further theoretical and experimental research.

References

[1] Ospelkaus S, Ni K K, Wang D, de M H G, Neyenhuis B, QuéQner G, Julienne P S, Bohn J L, Jin D S and Ye J 2010 *Science* **327** 853
[2] Krems R V 2008 *Phys. Chem. Chem. Phys.* **10** 4079
[3] Baron J, Campbell W C, Demille D, Doyle J M, Gabrielse G, Gurevich Y V, Hess P W, Hutzler N R, Kirilov E, Kozyryev I, O'Leary B R, Panda C D, Parsons M F, Petrik E S, Spaun B, Vutha A C and West A D 2014 *Science* **343** 269
[4] Demille D 2002 *Phys. Rev. Lett.* **88** 067901
[5] Krems R V 2008 *Phys. Chem. Chem. Phys.* **10** 4079
[6] Rosa M D D 2004 *Eur. Phys. J. D* **31** 395
[7] Shuman E S, Barry J F and Demille D 2010 *Nature* **467** 820
[8] Hummon M T, Yeo M, Stuhl B K, Collopy A L, Xia Y and Ye J 2013 *Phys. Rev. Lett.* **110** 143001
[9] Zhelyazkova V, Cournol A, Wall T E, Matsushima A, Hudson J J, Hinds E A, Tarbutt M R and Sauer B E 2014 *Phys. Rev. A* **89** 12707
[10] Hendricks R J, Holl, D A, Truppe S, Sauer B E and Tarbutt M R 2014 *Front. Phys.* **2** 51
[11] Tarallo M G, Iwata G Z and Zelevinsky T 2016 *Phys. Rev. A* **93** 032509
[12] Xu L, Yin Y, Wei B, Xia Y and Yin J P 2016 *Phys. Rev. A* **93** 39
[13] Gao Y F and Gao T 2014 *Phys. Rev. A* **90** 052506
[14] Zhang Y G, Zhang H and Dou G 2017 *Acta Phys. Sin.* **66** 233101 (in Chinese)
[15] Lane I C 2012 *Phys. Chem. Chem. Phys.* **14** 15078
[16] Cade P E and Huo W M 1967 *J. Chem. Phys.* **47** 649
[17] Wan M J, Shao J X, Huang D H, Jin C G, Yu Y and Wang F H 2015 *Phys. Chem. Chem. Phys.* **17** 26731
[18] Wells N and Lane I C 2011 *Phys. Chem. Chem. Phys.* **13** 19018
[19] Nguyen J H V and Odom B 2011 *Phys. Rev. A* **83** 053404
[20] Gao Y and Gao T 2015 *Phys. Chem. Chem. Phys.* **17** 10830
[21] McKellar A and Richardson E H 1955 *Astrophys. J.* **122** 196
[22] Chen P, Pallix J B, Chupks W A and Colson S D 1986 *J. Chem. Phys.* **84** 527
[23] Huber K P and Herzberg G 1979 *Molecular Spectra and Molecular Structure IV. Constants of Diatomic Molecules* (New York: Van Nostrand Reinhold Company Inc.)
[24] Kalemos A, Mavridis A and Metropoulos A 1999 *J. Chem. Phys.* **111** 9536
[25] Kleinschmidit M, Fleig T and Marian C M 2002 *J. Mol. Spectrosc.* **211** 179
[26] Hettema H and Yarkony D R 1994 *J. Chem. Phys.* **100** 8991
[27] Li Q and Zhu Z H 2006 *Acta Phys. Sin.* **55** 102 (in Chinese)
[28] Sun H and Freed K F 2003 *J. Chem. Phys.* **118** 8281
[29] Richards W G and Cooper D L 1981 *J. Phys. B: At. Mol. Phys.* **14** L131
[30] Zachwieja M 1995 *J. Mol. Spectrosc.* **170** 285
[31] Kasdan A, Herbst E and Lineberger W C 1975 *Chem. Phys. Lett.* **31** 78
[32] kepa R, Para A, Rytel M and Zachwieja M 1996 *J. Mol. Spectrosc.* **178** 189
[33] Kumar A, Hsiao C C, Hung W C and Lee Y P 1998 *J. Chem. Phys.* **109** 3824
[34] Herzberg G and Johns J W C 1969 *Astrophys. J.* **158** 399
[35] Werner H J, Knowles P J, Lindh R, Knizia G, Manby F R and Schütz M 2010 "MOLPRO Version 2010.1, a package of *ab initio* programs," see http://www.molpro.net
[36] Knowles P J and Werner H J 1985 *J. Chem. Phys.* **82** 5053
[37] Knowles P J and Werner H J 1985 *Chem. Phys. Lett.* **115** 259
[38] Xia W, Fu M, Ma H and Bian W 2017 *Chem. Phys.* **485** 29
[39] Werner H J and Knowles P J 1988 *J. Chem. Phys.* **89** 5803
[40] Knowles P J and Werner H J 1988 *Chem. Phys. Lett.* **145** 514
[41] You Y, Yang C L, Wang M S, Ma X G and Liu W W 2015 *Phys. Rev. A* **92** 032502
[42] Laughoff S R and Davidson E R 1974 *Int. J. Quantum Chem.* **8** 61
[43] Douglas N and Kroll N M 1974 *Ann. Phys.* **82** 89
[44] Hess B A 1986 *Phys. Rev. A* **33** 3742
[45] Di Rosa M D 2004 *Eur. Phys. J. D-At. Mol. Opt. Plasma Phys.* **31** 395
[46] Le Roy R J 2015 "LEVEL 8.2: A computer program for solving the radial Schrödinger equation for bound and quasibound levels, Chemical Physics Research Report CP-668" (University of Waterloo)
[47] Herzberg G 1950 *Molecular spectra and molecular structure: spectra of diatomic molecules*, Vol. 1, **6** 273
[48] Zhang Y G, Zhang H, Song H Y, Yu Y and Wan M J 2017 *Phys. Chem. Chem. Phys.* **19** 24647
[49] Wan M J, Yuan D, Jin C G, Wang F H, Yang Y J, Yu Y and Shao J X 2016 *J. Chem. Phys.* **145** 341
[50] Fu M, Cao J, Ma H and Bian W 2016 *Rsc. Adv.* **6** 100568
[51] Fu M, Ma H, Cao J and Bian W 2016 *J. Chem. Phys.* **144** 184302
[52] Fu M, Ma H, Cao J and Bian W 2017 *J. Chem. Phys.* **146** 134309